Published in final edited form as:
Biol Psychiatry. 2008 April 15; 63(8): 759–765.

Effect of chronic antipsychotic exposure on astrocyte and oligodendrocyte numbers in macaque monkeys

Glenn T. Konopaske[1,4,5], **Karl-Anton Dorph-Petersen**[1,6], **Robert A. Sweet**[1], **Joseph N. Pierri**[1], **Wei Zhang**[3], **Allan R. Sampson**[3], and **David A. Lewis**[*,1,2]

1*Department of Psychiatry, University of Pittsburgh, Pittsburgh, PA, USA*

2*Department of Neuroscience, University of Pittsburgh, Pittsburgh, PA, USA*

3*Department of Statistics, University of Pittsburgh, Pittsburgh, PA, USA*

4*McLean Hospital, Belmont, MA, USA*

5*Department of Psychiatry, Harvard Medical School, Boston, MA, USA*

6*Center for Psychiatric Research, Aarhus University Hospital, Risskov, Denmark*

Abstract

Background—Both *in vivo* and post-mortem studies suggest that oligodendrocyte and myelination alterations are present in individuals with schizophrenia. However, it is unclear whether prolonged treatment with antipsychotic medications contributes to these disturbances. We recently reported that chronic exposure of macaque monkeys to haloperidol or olanzapine was associated with a 10−18% lower glial cell number in the parietal grey matter. Consequently, in this study we sought to determine whether the lower glial cell number was due to fewer oligodendrocytes as opposed to lower numbers of astrocytes.

Methods—Using fluorescent immunocytochemical techniques, we optimized the visualization of each cell type throughout the entire thickness of tissue sections, while minimizing final tissue shrinkage. As a result, we were able to obtain robust stereological estimates of total oligodendrocyte and astrocyte numbers in the parietal grey matter using the optical fractionator method.

Results—We found a significant 20.5% lower astrocyte number with a non-significant 12.9% lower oligodendrocyte number in the antipsychotic-exposed monkeys. Similar effects were seen in both the haloperidol and olanzapine groups.

Conclusion—These findings suggest that studies investigating glial cell alterations in schizophrenia must take into account the effect of antipsychotic treatment.

Keywords

macaque monkeys; haloperidol; olanzapine; oligodendrocyte; astrocyte; stereology

*Corresponding Author: David A. Lewis, M.D. W1650 BST Department of Psychiatry University of Pittsburgh 3811 O'Hara Street Pittsburgh, PA 15213 lewisda@upmc.edu +1 412−624−3934.

Financial Disclosures David Lewis has received research funding from Pfizer and Merck, has served as a consultant to Bristol-Meyer Squibb, Lilly, Pfizer, Roche, Sepracor, and Wyeth. Allan Sampson is a statistical consultant for Johnson & Johnson Pharmaceutical Research and Development LLC. All other authors report no biomedical financial interests or potential conflicts of interest

Introduction

Cognitive deficits, among the core clinical features of schizophrenia (1), appear to reflect dysfunction of a number of cortical regions. Oligodendrocytes, by ensheathing cortical axons with myelin, enhance the rate of action potential conduction along axons and thereby play an important role in cognitive functions (2;3). In individuals with schizophrenia, alterations in cortical myelination have been detected using MRI (4), and a lower number of oligodendrocytes has been found in the dorsolateral prefrontal cortex in post-mortem studies (5). Moreover, reduced levels of transcripts selectively expressed by oligodendrocytes have been reported in schizophrenia (6;7), and polymorphisms in the myelin-associated glycoprotein (MAG) gene have been associated with susceptibility to the illness (8). Together these studies suggest that subjects with schizophrenia have fewer oligodendrocytes and that those present are functionally impaired.

However, it remains unclear the degree to which chronic antipsychotic treatment contributes to lower oligodendrocyte numbers. We recently reported that chronic exposure to haloperidol and olanzapine in macaque monkeys is associated with a lower number of glial cells in the grey matter of the parietal lobe (9), which was selected for study because it was the brain regions with the greatest antipsychotic-associated volume decrement (10). Based upon the literature cited above, we hypothesized that the antipsychotic-associated lower glial cell number was due predominantly to fewer oligodendrocytes. To test this hypothesis we used methods, based upon unbiased stereological principles, to estimate the number of oligodendrocytes immunoreactive for myelin 2',3'-cyclic nucleotide 3'-phosphodiesterase (CNP), an enzyme specific to oligodendrocytes (11), and as a negative control, the number of astrocytes labeled for S100B, a calcium binding protein found mostly in astrocytes and in a small subset (~2%) of oligodendrocytes (12) in the same cohort of haloperidol-, olanzapine-, and sham-exposed monkeys used in our previous studies (9;10). To obtain robust estimates of cell numbers, we developed an approach to optimize the visualization of immunoreactive oligodendrocytes and astrocytes throughout the entire thickness of tissue sections while minimizing final tissue shrinkage.

Methods and Materials

Antipsychotic drug administration to monkeys

The procedures for the chronic exposure of macaque monkeys to antipsychotic medications, euthanasia, brain removal, and dissection were reported previously (10). All studies were carried out in accordance with the NIH Guide for the Care and Use of Laboratory Animals and were approved by the University of Pittsburgh Institutional Animal Care and Use Committee. In brief, 18 experimentally-naïve, sexually mature (4.5−5.3 years of age) male macaque monkeys (*Macaca fascicularis*) were divided into 3 groups (n = 6 monkeys / group). The mean initial and terminal body weights, along with the mean weight gain during the period of antipsychotic administration, did not differ across the three groups (10). Animals received twice daily oral doses of sweetened pellets containing haloperidol, olanzapine, or sham for 17 −27 months. At steady state, trough plasma levels of haloperidol and olanzapine were 1.5 and 15 ng/ml, respectively; values within the range of plasma levels reported to be effective in schizophrenia (13;14).

Tissue processing

Following antipsychotic medication exposure, monkeys were matched by terminal body weight and euthanized in triads. The parietal lobe was dissected out as described previously (10). The parietal lobes were placed in 4% paraformaldehyde for 48 hours, rinsed in a graded series of sucrose solutions, and stored in cryoprotectant at −30°C. Each parietal lobe was

embedded in 7% low-melt agarose (SeaPlaque Agarose, Cambrex, Rockland, ME) and cut (perpendicular to the intra-parietal sulcus) in a systematic, uniformly random manner producing 12−15 slabs with a mean thickness of $T = 2.5$ mm (see Fig. 1 in Ref. 15). The cutting was facilitated by the use of a knife which was custom-coated with a non-stick surface (STAR*COTE 7055, ICS Technologies, ON, Canada). Each monkey was assigned a coded number and the position of monkeys from each experimental group was randomized within individual triads. Each slab was mounted using the Precision Cryoembedding system (Pathology Innovations, Wyckoff, NJ) (16;17) and 40 μm sections (i.e., the block advance, $BA = 40$ μm), containing the full face of the slab, were cut from the rostral surface on a cryostat.

Tissue sections were incubated for 30 minutes at room temperature in phosphate buffered saline (PBS) containing 4.5% normal donkey serum and 4.5% normal human serum, and then incubated for 48 hours at 4°C in PBS containing 3% normal human serum, 3% normal donkey serum, 0.05% bovine serum albumin, and a mouse monoclonal antibody (SMI-91R, 1:1500 dilution; Covance Research Products, Berkeley, CA) directed against myelin 2,′3′-cyclic nucleotide 3′-phosphodiesterase (CNP) or a mouse monoclonal antibody (clone SH-B1, 1:16,000 dilution; Sigma-Aldrich, St. Louis, MO) directed against the beta subunit of the S-100 protein (S100B). Next, tissue sections were incubated for 24 hours at 4°C in PBS containing 3% normal human serum, 3% normal donkey serum, and a CY3-conjugated donkey anti-mouse antibody (1:400 dilution; Jackson ImmunoResearch Laboratories, West Grove, PA). Finally, all tissue sections were mounted on chrome alum-gelatin coated slides, air dried for <30 minutes, rehydrated for 10 minutes in distilled water, and coverslipped using ProLong Gold anti-fade medium (Molecular Probes, Eugene, OR). To optimize visualization of immunocreactive cells, tissue sections were pretreated with 1% sodium borohydrate for 1 hour for oligodendrocytes and 0.3% Triton X-100 was included in the blocking and both antibody incubation steps for astrocytes. Because Triton X-100 caused some oligodendrocytes to appear indistinct, it was not included in the oligodendrocyte incubation steps. One section from each slab of each animal was selected and processed for each antibody.

The CNP antibody has been shown to label oligodendrocytes (18) by specifically labeling the CNP protein as demonstrated by Western blot (19). Moreover, no immunoreactivity was detected in brain tissue sections from a CNP knock-out mouse (20). The S100B antibody has been shown to label astrocytes (21) by specifically labeling the beta subunit of the S-100 protein as demonstrated by Western blot (22). In addition, no immunoreactivity was detected in brain tissue sections from a S100B knock-out mouse (23).

Stereological assessment of CNP-IR oligodendrocyte and S100B-IR astrocyte number

A single investigator (GTK), blinded to experimental group and subject number, conducted all observations on the immunofluorescently-labeled sections using an Olympus BX51 microscope equipped with a MT1201 microcator (0.2 μm resolution), a ND281B readout (Heidenhain, Germany), and a X-Y-Z motorized specimen stage (ProScan, Prior Scientific, UK). A HQ TRITC filter (filter set 41002, excitation range = 510−560 nm, emission range = 573−648 nm, Chroma Technologies, Brattleboro, VT) was used with a 100W high pressure mercury burner (BH2-RFL-T3, Olympus, Japan) as a light source. Using a 2X photo eyepiece (PE2X, Olympus, Japan), a three-chip CCD camcorder (KY-F55B, JVC, Japan) was mounted on the top of the microscope, and forwarded a 760 × 570 pixels live image (50 frames/sec) to a personal computer. The computer ran the CAST stereology software package (Version 2.00.07, Olympus, Denmark), and was fitted with a frame grabber (Flashpoint 3D, Integral Technologies, IN) and a 19” monitor (FlexScan T765 Color Display Monitor, EIZO Nanao Corp., Japan) having a screen resolution of 1280 ×1024 pixels. The microscope was calibrated daily using a calibration slide, and was mounted on a vibration isolation table (Q500A, Qontrol Devices Inc., CA) to facilitate high magnification imaging.

A Plan Apo 4X objective was used to draw contours around the grey matter in each section. Using the cell soma as the sampling item, all CNP-immunoreactive (IR) oligodendrocytes (Figure 1) and S100B-IR astrocytes (Figure 2) were counted in optical disectors (24) using a Plan Apo 100X oil immersion objective (NA = 1.4) at a final magnification of 2677X at the monitor. To assess for intra-rater reliability of cell classification, 12 sections were arbitrarily selected from different monkeys. Cells were counted through the full thickness of each section twice on different days. The intra-class correlation coefficient across sections was 0.96 for both CNP-IR oligodendrocytes and S100B-IR astrocytes, demonstrating high intra-rater reliability.

In an initial calibration study, CNP-IR oligodendrocytes and S100B-IR astrocytes cells were sampled using unbiased counting frames (25) in the full thickness of 50 sections from two monkeys. A total of 1378 CNP-IR oligodendrocytes and 2284 S100B-IR astrocytes were counted, the z-position (i.e., the distance from the section surface) of each counted cell was recorded, and section thickness was measured at every frame containing a counted cell. Plots of the count data versus z-position revealed that CNP-IR oligodendrocytes and S100B-IR astrocytes could be visualized throughout the entire thickness of the tissue sections. In addition, local shrinkage was found to be linear such that a constant average cell density was observed at all levels of focus except at the surface of the sections corresponding to lost caps (26;27).

Based on these calibration data, the optical fractionator (28) was used to estimate the total numbers of CNP-IR oligodendrocytes and S100B-IR astrocytes in the grey matter of the left parietal lobe from all monkeys using an unbiased counting frame with an area of a_{frame} = 1318 μm^2, a disector height of h = 10 μm for CNP and h = 8 μm for S100B, and an upper guard zone of 6 μm for CNP and 4 μm for S100B. The disector height and upper guard zone were different for CNP and S100B sections because the calibration revealed different mean tissue section thickness for each set of sections (28.9 μm for CNP, 24.8 μm for S100B). Counting frames were arranged in a square grid, the distance between frames (i.e., the "stepping distance"), *D*, was different for CNP and S100B sections, but was kept constant for all the CNP and S100B sections within each monkey such that *D* varied from 500 to 900 μm for CNP and 1000 to 1150 μm for S100B sections across monkeys. *D* was adjusted for each monkey using the point count-based volume estimates obtained previously (9;10) and mean cell densities observed in preceding monkeys (calibration values were used for the first monkey) to achieve counts of at least 400 cells for both CNP-IR oligodendrocytes and S100B-IR astrocytes in each monkey. As a result, an average of 602 CNP-IR oligodendrocytes, and 525 S100B-IR astrocytes were counted in each monkey.

Similar to the calibration study, section thickness was measured at each frame containing a counted cell. For CNP, the mean section thickness across all sections was 29.4 μm with a mean coefficient of variation (*CV*) of 0.15 within each monkey and a mean *CV* of 0.05 across all monkeys. For S100B, the mean section thickness across all sections was 26.4 μm with a mean *CV* of 0.15 within each monkey and a mean *CV* of 0.06 across all monkeys. Thus, despite a high degree of variability in thickness within each section, which is commonly seen in cryostat sections, mean section thickness was stable across monkeys.

Uneven shrinkage in section thickness can introduce biases when using the classical optical fractionator. However, such potential biases were eliminated by using the optical fractionator based on a mean section thickness that was number-weighted ($\bar{t}_{Q^-}$) (26;27). Mean section thickness was number-weighted as follows: $\bar{t}_{Q^-} = \sum_i \left(t_i q_i^-\right) / \sum_i q_i^-$ where t_i is the local section thickness in the center of the *i*th counting frame having a count of q_i^- (26). Total cell numbers were estimated as: $N := \frac{1}{ssf} \cdot \frac{1}{asf} \cdot \frac{1}{hsf} \cdot \sum Q^-$ where *ssf* is the section sampling fraction

($\underline{BA/T}$), *asf* is the area sampling fraction (a_{frame}/D^2), *hsf* is the height sampling fraction ($h/\underline{t}_{Q^-}$), and Q^- is the number of a given cell type counted.

Precision of stereological estimates

The statistical power to discriminate group differences depends upon the number of animals in each group as well as the inter-individual variance within each group. Typically, the most efficient way to increase statistical power is by increasing subject number (29). However, in this study the number of available monkeys was limited. Because we used unbiased methods, the observed inter-individual variance is the sum of the genuine biological variance (i.e., the differences between animals if we could exactly determine the total number of the cells of interest) and the mean estimator variance (the stereological or methodological error). In many stereological studies, the estimator variance is a substantial fraction (25−50%) of the observed variance. Therefore, a minor gain in power can be obtained by further reducing the stereological method error. Thus, we used a large number of sections (~13 per monkey) and substantial cell counts for CNP-IR oligodendrocytes (~600 per monkey) and S100B-IR astrocytes (~500 per monkey) to produce stereological estimates with a high precision (Table 1). The precision of the number estimates were calculated using previously described methods (30). Due to the high precision of the stereological estimates, ~90% of the total observed variance within groups is due to variability in intrinsic biology across monkeys. Some additional variance might have been introduced due to immunofluorescent processing.

As reported previously (9), the parietal lobe was defined by anatomical boundaries to reduce the variability of brain region delineation. This decision was based on previous findings that the use of cytoarchitectonic boundaries does not increase the precision of brain region delineation because such delineations are associated with increased variability (31;32). In addition, this approach ensures that a brain region's delineation remains constant across measurements (e.g., brain region volume estimates *vs.* cell number estimates).

Statistical analyses

Because both haloperidol and olanzapine affected glial number to a similar degree (9), the contrast of the combined antipsychotic-exposed group versus the sham group, based upon a two-way ANOVA model (with additive effects of group and triad), was used to assess the effect of chronic antipsychotic exposure on the oligodendrocyte and astrocyte number and density measured for each monkey, and the ratio for each monkey of oligodendrocyte and astrocyte number to the total glial cell number previously estimated (9). One-sided testing of these contrasts was done due to the directionality of the hypothesized effect (e.g., reduced oligodendrocyte in antipsychotic-exposed monkeys). Analyses were implemented in SPSS and SAS PROC GLM with $\mu = 0.05$.

Results

In the grey matter of the left parietal lobe from antipsychotic-exposed monkeys, a 12.9% lower number of CNP-IR oligodendrocytes (Figure 3), relative to sham-exposed monkeys, trended toward significance ($t = -1.45$, $df = 10$, $p = 0.088$). In contrast, the number of S100B-IR astrocytes was significantly ($t = -2.05$, $df = 10$, $p = 0.034$) 20.5% lower (Figure 4) in the antipsychotic-exposed than in the sham-exposed group. Because chronic antipsychotic exposure was shown previously to be associated with a smaller volume of the parietal grey matter (9;10), the cell densities of CNP-IR oligodendrocytes and S100B-IR astrocytes were assessed and found not to be different from the sham-exposed group (CNP: $t = -0.08$, $df = 10$, $p = 0.47$; S100B: $t = -0.99$, $df = 10$, $p = 0.17$). To determine if chronic antipsychotic exposure altered the percentage of total glial cells attributable to oligodendrocytes or astrocytes, the ratios of CNP-IR oligodendrocyte number and of S100B-IR astrocyte number to the previously

reported total glial cell number were assessed and found not to differ from the sham-exposed group (CNP: t = 0.13, df = 10, $p = 0.55$; S100B: t = −0.72, df = 10, $p = 0.24$). Similar effects were also observed when the haloperidol- and olanzapine-exposed groups were individually compared to the sham group (Table 2).

Discussion

In contrast to our hypothesis, this study demonstrates that the lower grey matter glial cell number associated with chronic haloperidol and olanzapine exposure in macaque monkeys (9) is due mainly to a lower astrocyte number, whereas oligodendrocyte number appears to be affected to a smaller degree. Thus, these findings provide only weak support of the interpretation that the findings of lower oligodendrocyte number in schizophrenia are attributable to antipsychotic medications. Although these findings might not be generalizable to all antipsychotics, it is important to note that both haloperidol and olanzapine, despite having very different receptor binding profiles (33), produced similar effects on brain weight and volumes (10), glial cell number (34), and now astrocyte number. Therefore, it might be that treatment-associated lower astrocyte number is a common feature of both typical and atypical antipsychotic medications. Furthermore, given the role of astrocytes in glutamate homeostasis (35), an antipsychotic-associated lower astrocyte number might be of importance in interpreting studies investigating the role of this neurotransmitter system in the disease process of schizophrenia (36;37).

The synthesis and metabolism of glutamate in the neocortex involves trafficking of precursors and metabolites between neuronal and astrocytic compartments (35). After the release of glutamate from the presynaptic terminal, neurotransmission is terminated by the uptake of glutamate via high affinity transporters (EAAT1−5) (38). EAAT1 and 2 account for the bulk of glutamate transport in the brain (39) and are localized almost exclusively on astrocytes (40;41). Inside the astrocyte, glutamate is converted to glutamine via glutamine synthetase, an enzyme also localized almost exclusively to astrocytes (42). Glutamine is shuttled to neurons via a pathway mediated by system N transport (SN1) in astrocytes and system A transport (SAT/ATA) in neurons (43). Within neurons, glutamine is converted back to glutamate via phosphate-activated glutaminase (PAG) (38). Thus, lower astrocyte number following chronic antipsychotic exposure might affect cortical glutamate and glutamine levels.

Cortical glutamate and glutamine have been assessed *in vivo* using magnetic resonance spectroscopy (MRS) in antipsychotic-naïve (44) and chronically-ill (45) schizophrenia subjects. In the antipsychotic-naïve subjects, glutamate levels were unchanged in the anterior cingulate cortex (ACC), whereas glutamine levels were increased (44). In subjects with chronic schizophrenia both glutamate and glutamine levels were decreased in the ACC (45). Although disease progression might play a role, these MRS studies raise the possibility that an antipsychotic-mediated reduction in astrocyte number might contribute to lower glutamate and glutamine levels in the frontal cortex of subjects with schizophrenia. Although astrocyte number has not been assessed in the frontal lobe, chronic exposure to antipsychotics in the same monkeys was associated with similar volume decrements in both the parietal and frontal lobes (10) suggesting that similar effects on astrocyte number, and consequently, glutamate homeostasis might also occur in both brain regions.

The results of the current study raise the question of whether the lower number of S100B-IR astrocytes and CNP-IR oligodendrocytes accounts for the 14.2% lower total glial cell number observed previously in the antipsychotic-exposed monkeys (9). We previously estimated the mean total glial cell number in Nissl-stained tissue sections from the sham monkeys to be 175.3×10^6 cells; thus, the mean glial cell number was 14.2% lower in the antipsychotic-exposed monkeys, corresponding to ~ 25.0×10^6 fewer glial cells. Here, in sham monkeys, we

estimated the mean number of S100B-IR astrocytes to be 90.9×10^6 cells and the mean number of CNP-IR oligodendrocytes to be 47.8×10^6 cells (Table 1). In the antipsychotic-exposed monkeys, we estimated the mean numbers of S100B-IR astrocytes and CNPIR oligodendrocytes to be 20.5% and 12.9% lower relative to the sham monkeys (Table 2) corresponding to 18.6×10^6 fewer S100B-IR cells and 6.2×10^6 fewer CNP-IR or a total of $\sim24.8\times10^6$ fewer immunoreactive cells. Interestingly, this lower number of immunoreactive cells is virtually identical to the observed lower total Nissl-stained glial cell number suggesting that the differences in S100B-IR and CNP-IR cell number across groups reflect a lower number of cells in the antipsychotic-exposed monkeys. Nevertheless, although unlikely, we cannot entirely exclude the possibility that an antipsychotic-associated loss of immunoreactivity might contribute, at least in part, to the apparent lower number of S100B-IR and CNP-IR cells.

This study also reports methods which ensured adequate visualization of immunoreactive oligodendrocytes and astrocytes throughout the entire thickness of tissue sections while minimizing final tissue shrinkage; both of these factors are critical to obtain robust and unbiased estimates of total cell number. Immunocytochemical methods using diaminobenzidene (DAB) as a chromogen can be hampered by the incomplete visualization of labeled structures in the middle of tissue sections, perhaps due to inability of DAB to polymerize to an adequate amount throughout the entire section thickness. On the other hand, immunofluorescent methods, with careful selection of antibodies and minor modifications to the tissue processing methods (e.g., inclusion or exclusion of Triton X-100), can circumvent this handicap. In addition to the improved visualization, our current methods also included a rehydration step prior to the application of a coverslip which, combined with a section drying time of <30 minutes (27; 46), limits the degree of final tissue shrinkage (e.g., ~30% for immunofluorescence, see also Ref. 47). Minimizing final tissue shrinkage enhances the spatial discrimination among neighboring cells and increases the efficiency of cell counting by reducing the number of counting sites required.

In summary, the findings of this study indicate that chronic exposure to haloperidol and olanzapine is associated with significantly lower astrocyte number in the parietal cortex. Since fewer astrocytes might impact the synthesis, metabolism, and neurotransmission of cortical glutamate, this study suggests that both *in vivo* imaging and post-mortem studies of the glutamate system in schizophrenia should control for the possible confounding effect of chronic antipsychotic treatment. In addition, this study illustrates the use of methods which allowed robust and efficient stereological number estimates of immunofluorescently-labeled cells in the CNS and have relevance to experiments conducted in diverse areas of neuroscience.

Acknowledgements

We thank Susan Konopaske and Dost Öngür for helpful comments to this paper and Mary Brady for help with graphics. The study received support from Eli Lilly and Company and NIH Grants MH45156, MH01945, MH71533, and MH16804.

References

1. Elvevåg B, Goldberg TE. Cognitive impairment in schizophrenia is the core of the disorder. Crit Rev Neurobiol 2000;14:1–21. [PubMed: 11253953]
2. Atkins CM, Chen SJ, Klann E, Sweatt JD. Increased phosphorylation of myelin basic protein during hippocampal long-term potentiation. J Neurochem 1997;68:1960–1967. [PubMed: 9109522]
3. Comi G, Filippi M, Martinelli V, Sirabian G, Visciani A, Campi A, et al. Brain magnetic resonance imaging correlates of cognitive impairment in multiple sclerosis. J Neurol Sci 1993;115(Suppl):S66–S73. [PubMed: 8340796]
4. Flynn SW, Lang DJ, Mackay AL, Goghari V, Vavasour IM, Whittall KP, et al. Abnormalities of myelination in schizophrenia detected in vivo with MRI, and post-mortem with analysis of oligodendrocyte proteins. Mol Psychiatry 2003;8:811–820. [PubMed: 12931208]

5. Hof PR, Haroutunian V, Friedrich VL Jr. Byne W, Buitron C, Perl DP, et al. Loss and altered spatial distribution of oligodendrocytes in the superior frontal gyrus in schizophrenia. Biol Psychiatry 2003;53:1075–1085. [PubMed: 12814859]
6. Hakak Y, Walker JR, Li C, Wong WH, Davis KL, Buxbaum JD, et al. Genome-wide expression analysis reveals dysregulation of myelination-related genes in chronic schizophrenia. Proc Natl Acad Sci USA 2001;98:4746–4751. [PubMed: 11296301]
7. Tkachev D, Mimmack ML, Ryan MM, Wayland M, Freeman T, Jones PB, et al. Oligodendrocyte dysfunction in schizophrenia and bipolar disorder. Lancet 2003;362:798–805. [PubMed: 13678875]
8. Yang YF, Qin W, Shugart YY, He G, Liu XM, Zhou J, et al. Possible association of the MAG locus with schizophrenia in a chinese han cohort of family trios. Schizophr Res 2005;75:11–19. [PubMed: 15820319]
9. Konopaske GT, Dorph-Petersen KA, Pierri JN, Wu Q, Sampson AR, Lewis DA. Effect of chronic exposure to antipsychotic medication on cell numbers in the parietal cortex of macaque monkeys. Neuropsychopharmacol 2007;32:1216–1223.
10. Dorph-Petersen KA, Pierri JN, Perel JM, Sun Z, Sampson AR, Lewis DA. The influence of chronic exposure to antipsychotic medications on brain size before and after tissue fixation: a comparison of haloperidol and olanzapine in macaque monkeys. Neuropsychopharmacol 2005;30:1649–1661.
11. Vogel US, Reynolds R, Thompson RJ, Wilkin GP. Expression of the 2′,3′-cyclic nucleotide 3′-phosphohydrolase gene and immunoreactive protein in oligodendrocytes as revealed by in situ hybridization and immunofluorescence. Glia 1988;1:184–190. [PubMed: 2852171]
12. Rickmann M, Wolff JR. S100 immunoreactivity in a subpopulation of oligodendrocytes and Ranvier's nodes of adult rat brain. Neurosci Lett 1995;186:13–16. [PubMed: 7783941]
13. Oosthuizen P, Emsley R, Jadri Turner H, Keyter N. A randomized, controlled comparison of the efficacy and tolerability of low and high doses of haloperidol in the treatment of first-episode psychosis. Int J Neuropsychopharmacol 2004;7:125–131. [PubMed: 15003147]
14. Perry PJ, Lund BC, Sanger T, Beasley C. Olanzapine plasma concentrations and clinical response: acute phase results of the North American Olanzapine Trial. J Clin Psychopharmacol 2001;21:14–20. [PubMed: 11199942]
15. Baddeley A, Dorph-Petersen KA, Vedel Jensen EB. A note on the stereological implications of irregular spacing of sections. J Microsc 2006;222:177–181. [PubMed: 16872416]
16. Peters SR. The art of embedding tissue for frozen section. part i: a system for face down cryoembedding of tissues using freezing temperature embedding wells. J Histotechnol 2003;26:11–19.
17. Peters SR. The art of embedding tissue for frozen section. part ii: frozen block cryoembedding. J Histotechnol 2003;26:23–28.
18. Windrem MS, Roy NS, Wang J, Nunes M, Benraiss A, Goodman R, et al. Progenitor cells derived from the adult human subcortical white matter disperse and differentiate as oligodendrocytes within demyelinated lesions of the rat brain. J Neurosci Res 2002;69:966–975. [PubMed: 12205690]
19. McFerran B, Burgoyne R. 2′,3′-cyclic nucleotide 3′-phosphodiesterase is associated with mitochondria in diverse adrenal cell types. J Cell Sci 1997;110:2979–2985. [PubMed: 9359886]
20. Lappe-Siefke C, Goebbels S, Gravel M, Nicksch E, Lee J, Braun PE, et al. Disruption of Cnp1 uncouples oligodendroglial functions in axonal support and myelination. Nat Genet 2003;33:366–374. [PubMed: 12590258]
21. Kofler B, Bulleyment A, Humphries A, Carter DA. Id-1 expression defines a subset of vimentin/S-100beta-positive, GFAP-negative astrocytes in the adult rat pineal gland. Histochem J 2002;34:167–171. [PubMed: 12495223]
22. Yu WH, Fraser PE. S100beta interaction with tau is promoted by zinc and inhibited by hyperphosphorylation in Alzheimer's disease. J Neurosci 2001;21:2240–2246. [PubMed: 11264299]
23. Nishiyama H, Takemura M, Takeda T, Itohara S. Normal development of serotonergic neurons in mice lacking S100B. Neurosci Lett 2002;321:49–52. [PubMed: 11872254]
24. Gundersen HJG. Stereology of arbitrary particles. A review of unbiased number and size estimators and the presentation of some new ones in the memory of William R. Thompson. J Microsc 1986;143:3–45. [PubMed: 3761363]

25. Gundersen HJG. Notes on the estimation of the numerical density of arbitrary profiles: the edge effect. J Microsc 1977;111:219–223.
26. Dorph-Petersen, KA. Ph.D. Thesis. University of Aarhus. 2001. Neuronal changes in the dorsal raphe nucleus in depression..
27. Dorph-Petersen, KA.; Rosenberg, R.; Nyengaard, JR. Estimation of number and volume of immunohistochemically stained neurons in complex brain regions.. In: Evans, SM.; Janson, AM.; Nyengaard, JR., editors. Quantitative methods in neuroscience. Oxford University Press; Oxford: 2004. p. 216-238.
28. West MJ, Slomianka L, Gundersen HJG. Unbiased stereological estimation of the total number of neurons in the subdivisions of the rat hippocampus using the optical fractionator. Anat Rec 1991;231:482–497. [PubMed: 1793176]
29. Gundersen HJG, Østerby R. Optimizing sampling efficiency of stereological studies in biology: or 'do more less well!'. J Microsc 1981;121:65–73. [PubMed: 7014910]
30. Gundersen HJG, Jensen EBV, Kiêu K, Nielsen J. The efficiency of systematic sampling in stereology--reconsidered. J Microsc 1999;193:199–211. [PubMed: 10348656]
31. Dorph-Petersen KA, Pierri JN, Sun Z, Sampson AR, Lewis DA. Stereological analysis of the mediodorsal thalamic nucleus in schizophrenia: volume, neuron number, and cell types. J Comp Neurol 2004;472:449–62. [PubMed: 15065119]
32. Sweet RA, Dorph-Petersen KA, Lewis DA. Mapping auditory core, lateral belt, and parabelt cortices in the human superior temporal gyrus. J Comp Neurol 2005;491:270–89. [PubMed: 16134138]
33. Zhang W, Bymaster FP. The in vivo effects of olanzapine and other antipsychotic agents on receptor occupancy and antagonism of dopamine D1, D2, D3, 5HT2A and muscarinic receptors. Psychopharmacology (Berl) 1999;141:267–78. [PubMed: 10027508]
34. Konopaske, GT.; Dorph-Petersen, KA.; Lewis, DA. Poster Presentation. Society for Neuroscience Annual Meeting; Atlanta, GA: 2006. Effect of chronic exposure to antipsychotic medications on glial cell numbers in the parietal cortex of macaque monkeys.
35. Hertz L. Intercellular metabolic compartmentation in the brain: past, present and future. Neurochem Int 2004;45:285–296. [PubMed: 15145544]
36. Coyle JT. The GABA-glutamate connection in schizophrenia: which is the proximate cause? Biochem Pharmacol 2004;68:1507–1514. [PubMed: 15451393]
37. Lewis DA, Gonzalez-Burgos G. Pathophysiologically based treatment interventions in schizophrenia. Nat Med 2006;12:1016–1022. [PubMed: 16960576]
38. Bak LK, Schousboe A, Waagepetersen HS. The glutamate/GABA-glutamine cycle: aspects of transport, neurotransmitter homeostasis and ammonia transfer. J Neurochem 2006;98:641–653. [PubMed: 16787421]
39. Schousboe A, Sarup A, Bak LK, Waagepetersen HS, Larsson OM. Role of astrocytic transport processes in glutamatergic and GABAergic neurotransmission. Neurochem Int 2004;45:521–527. [PubMed: 15186918]
40. Chaudhry FA, Lehre KP, van Lookeren Campagne M, Ottersen OP, Danbolt NC, Storm-Mathisen J. Glutamate transporters in glial plasma membranes: highly differentiated localizations revealed by quantitative ultrastructural immunocytochemistry. Neuron 1995;15:711–720. [PubMed: 7546749]
41. Rothstein JD, Martin L, Levey AI, Dykes-Hoberg M, Jin L, Wu D, et al. Localization of neuronal and glial glutamate transporters. Neuron 1994;13:713–725. [PubMed: 7917301]
42. Norenberg MD, Martinez-Hernandez A. Fine structural localization of glutamine synthetase in astrocytes of rat brain. Brain Res 1979;161:303–310. [PubMed: 31966]
43. Bröer S, Brookes N. Transfer of glutamine between astrocytes and neurons. J Neurochem 2001;77:705–719. [PubMed: 11331400]
44. Théberge J, Bartha R, Drost DJ, Menon RS, Malla A, Takhar J, et al. Glutamate and glutamine measured with 4.0 T proton MRS in never-treated patients with schizophrenia and healthy volunteers. Am J Psychiatry 2002;159:1944–1946. [PubMed: 12411236]
45. Théberge J, Al-Semaan Y, Williamson PC, Menon RS, Neufeld RW, Rajakumar N, et al. Glutamate and glutamine in the anterior cingulate and thalamus of medicated patients with chronic schizophrenia and healthy comparison subjects measured with 4.0-T proton MRS. Am J Psychiatry 2003;160:2231–2233. [PubMed: 14638596]

46. Dorph-Petersen KA, Nyengaard JR, Gundersen HJG. Tissue shrinkage and unbiased stereological estimation of particle number and size. J Microsc 2001;204:232–246. [PubMed: 11903800]

47. Peterson, DA. The use of fluorescent probes in cell-counting procedures.. In: Evans, SM.; Janson, AM.; Nyengaard, JR., editors. Quantitative methods in neuroscience. Oxford University Press; Oxford: 2004. p. 86-114.

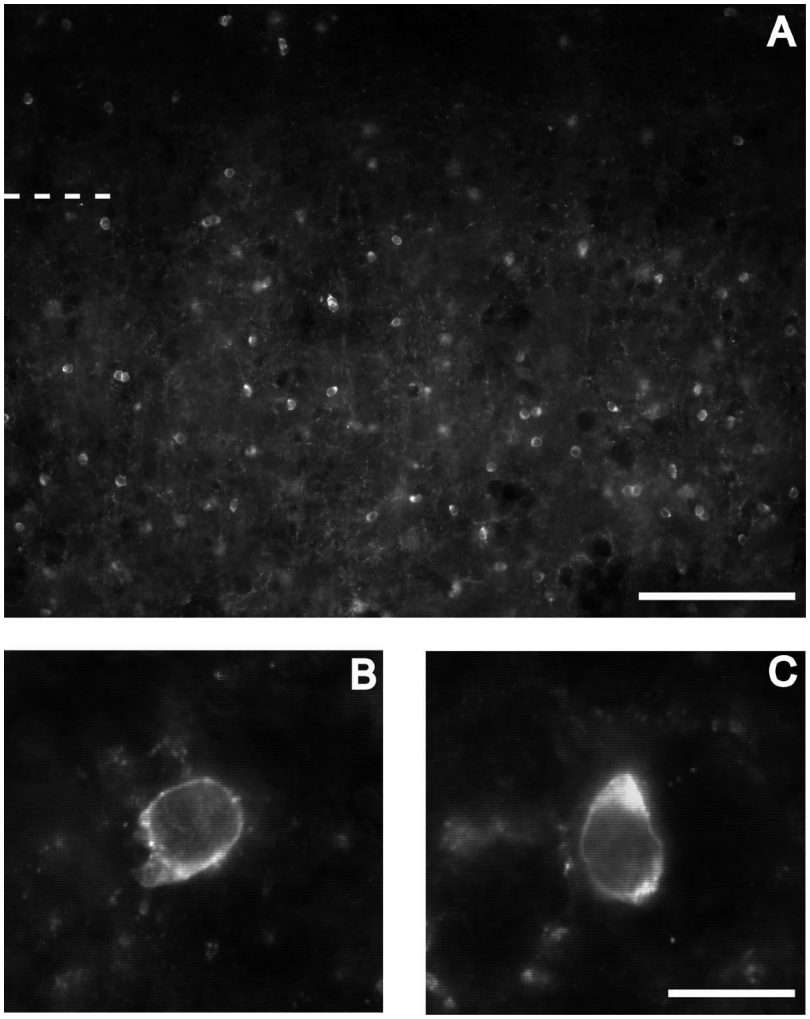

Figure 1.
Epifluorescent photomicrographs of CNP-IR oligodendrocytes. Panel A: Low-power (20X) photomicrograph demonstrating the distribution of CNP-IR oligodendrocytes in the superficial cortical layers of the parietal lobe. Dashed line indicates the layer 1−2 border. Calibration bar = 150 μm. Panels B & C: High power (100X) photomicrographs demonstrating typical somal morphology of CNP-IR oligodendrocytes. Calibration bar = 10 μm.

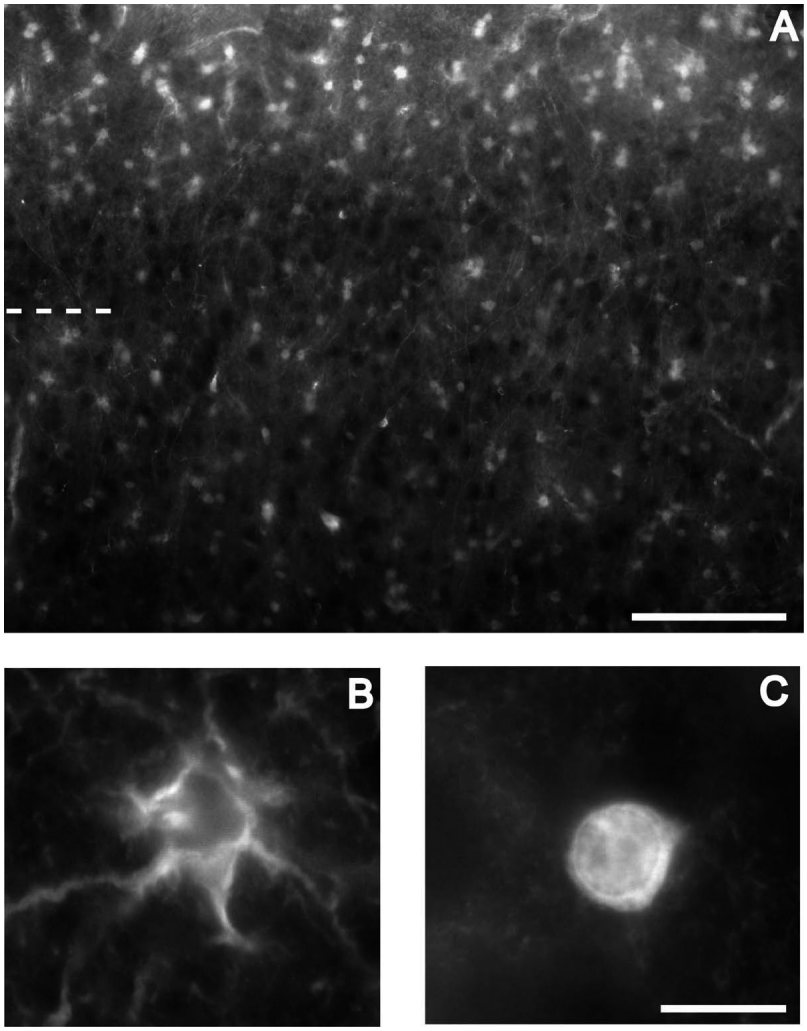

Figure 2.
Epifluorescent photomicrographs of S100B-IR astrocytes. Panel A: Low-power (20X) photomicrograph demonstrating the distribution of S100B-IR astrocytes in the superficial cortical layers of the parietal lobe. Dashed line indicates the layer 1−2 border. Calibration bar = 150 μm. Panels B & C: High power (100X) photomicrographs demonstrating typical somal morphology of S100B-IR astrocytes. Calibration bar = 10 μm.

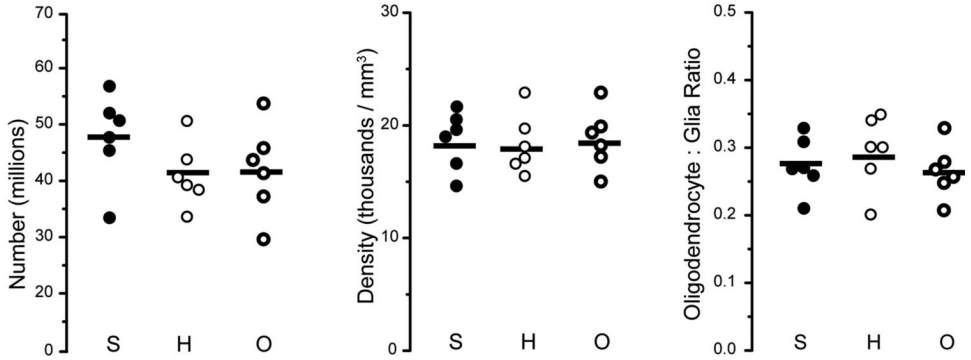

Figure 3.

CNP-IR oligodendrocyte cell number, density, and CNP-IR oligodendrocyte number : total glial cell number ratio from the left parietal lobe of the haloperidol- (thin open circles), olanzapine- (thick open circles), and sham- (filled circles) exposed monkeys. No significant differences were detected between groups. The horizontal bars indicate sham and antipsychotic-exposed group means.

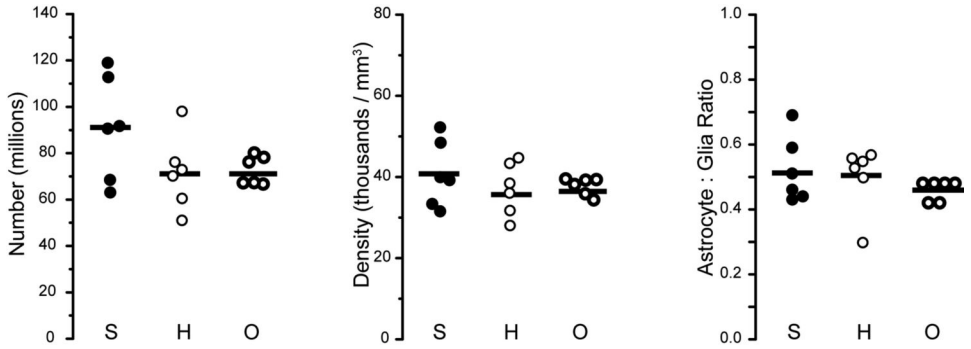

Figure 4.

S100B-IR astrocyte cell number, density, and S100B-IR astrocyte number : total glial cell number ratio from the left parietal lobe of the haloperidol- (thin open circles), olanzapine- (thick open circles), and sham- (filled circles) exposed monkeys. The number of S100B-IR astrocytes significantly differed between the antipsychotic-exposed and sham groups (p = 0.034). The horizontal bars indicate sham and antipsychotic-exposed group means.

Table 1

Summary of Stereological Results

	N_{oligo} (x 10^6)	(CE)	N_{astro} (x 10^6)	(CE)
Sham				
Mean	47.8	(0.04)	90.9	(0.04)
SD	8.1		22.6	
CV	0.17		0.25	
Antipsychotic-exposed				
Mean	41.6	(0.05)	72.3	(0.05)
SD	6.7		11.6	
CV	0.16		0.16	

N_{oligo} is the total number of CNP-IR oligodendrocytes, and N_{astro} is the total number of S100B-IR astrocytes. Standard deviation (SD), mean coefficient of error (*CE*), and interindividual coefficient of variation (*CV*) are listed for all measures.

Table 2

Comparison of Antipsychotic Groups with Sham

	All antipsychotics		Haloperidol		Olanzapine	
	Mean % difference	***p***	**Mean % difference**	***p***	**Mean % difference**	***p***
Oligodendrocyte number	−12.9%	0.088	−13.9%	0.1	−11.8%	0.14
Astrocyte number	−20.5%	0.034	−20.4%	0.053	−20.5%	0.053
Oligodendrocyte density	−0.7%	0.47	−1.7%	0.43	0.4%	0.48
Astrocyte density	−8.3%	0.17	−9.2%	0.18	−7.4%	0.23
Oligo:Glia ratio	1.2%	0.45	5.7%	0.31	−3.3%	0.39
Astro:Glia ratio	−6.8%	0.24	−2.1%	0.43	−11.5%	0.16

p-values represent the results of a two-way ANOVA model followed by a one-tailed contrast of the indicated antipsychotic group and sham group.